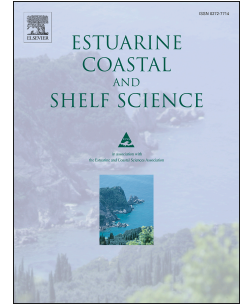


# Journal Pre-proof

Ungrazed salt marsh has well connected soil pores and less dense sediment compared with grazed salt marsh: CT scanning study

Amr Keshta, Ketil Koop-Jakobsen, Jürgen Titschack, Peter Mueller, Kai Jensen, Andrew Baldwin, Stefanie Nolte



PII: S0272-7714(20)30718-6

DOI: <https://doi.org/10.1016/j.ecss.2020.106987>

Reference: YECSS 106987

To appear in: *Estuarine, Coastal and Shelf Science*

Received Date: 29 March 2020

Revised Date: 2 August 2020

Accepted Date: 4 August 2020

Please cite this article as: Keshta, A., Koop-Jakobsen, K., Titschack, Jü., Mueller, P., Jensen, K., Baldwin, A., Nolte, S., Ungrazed salt marsh has well connected soil pores and less dense sediment compared with grazed salt marsh: CT scanning study, *Estuarine, Coastal and Shelf Science* (2020), doi: <https://doi.org/10.1016/j.ecss.2020.106987>.

This is a PDF file of an article that has undergone enhancements after acceptance, such as the addition of a cover page and metadata, and formatting for readability, but it is not yet the definitive version of record. This version will undergo additional copyediting, typesetting and review before it is published in its final form, but we are providing this version to give early visibility of the article. Please note that, during the production process, errors may be discovered which could affect the content, and all legal disclaimers that apply to the journal pertain.

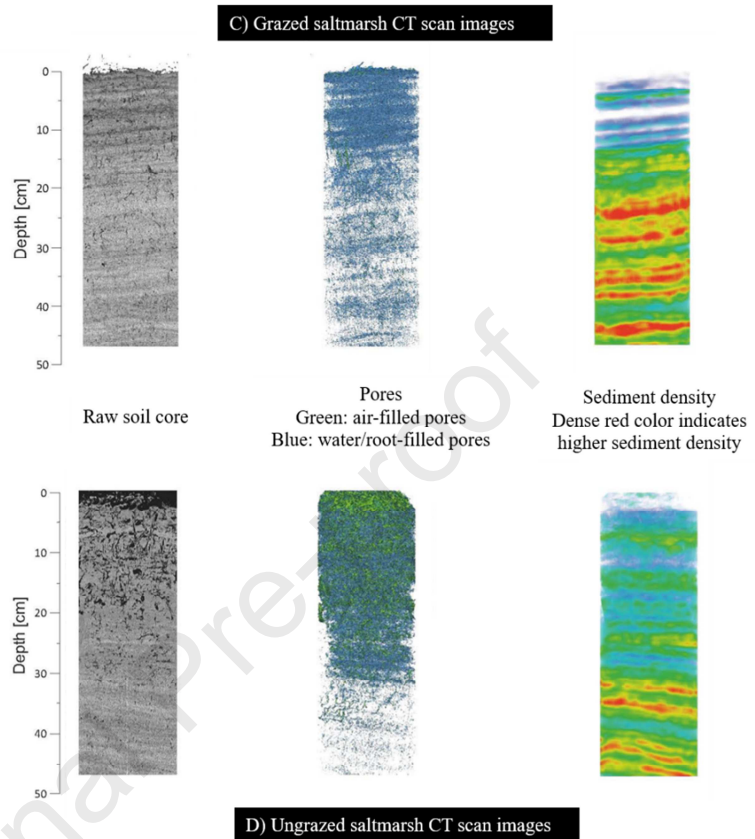
© 2020 Published by Elsevier Ltd.

**Author contributions statement**

SN, PM, and KJ designed the original study setup with further contributions from AK, KKJ, and AB. JT conducted the CT scans and supervised AK in data processing. Lab measurements were done by AK, with contributions to grain size analysis by KKJ and JT. AK analyzed results and wrote the main draft of the manuscript. All authors contributed to the discussion of results and the writing of the manuscript.

Journal Pre-proof

Graphical abstract



1 **Title**

2 Ungrazed salt marsh has well connected soil pores and less dense sediment compared with grazed salt marsh:  
3 CT scanning study

4 **Authors and addresses**

5 Amr Keshta<sup>1,2,\*</sup>, Ketil Koop-Jakobsen<sup>3,4</sup>, Jürgen Titschack<sup>4,5</sup>, Peter Mueller<sup>6</sup>, Kai Jensen<sup>7</sup>, Andrew Baldwin<sup>2</sup>,  
6 and Stefanie Nolte<sup>8,9</sup>

7 <sup>1</sup> Botany Department, College of Science, Tanta University, 3111 Tanta, Egypt

8 <sup>2</sup> Department of Environmental Science and Technology, University of Maryland, College Park, Maryland  
9 20742, USA

10 <sup>3</sup> The Alfred Wegener Institute, Helmholtz Centre for Polar and Marine Research, Wadden Sea Station, D-  
11 25992, Germany

12 <sup>4</sup> MARUM – Center for Marine Environmental Sciences, University of Bremen, Bremen, Germany

13 <sup>5</sup> Senckenberg am Meer, Marine Research Department, 26382 Wilhelmshaven, Germany

14 <sup>6</sup> Smithsonian Environmental Research Center, 647 Contees Wharf Rd, Edgewater, MD 21037, United States

15 <sup>7</sup> Applied Plant Ecology, Institute for Plant Sciences and Microbiology, Universität Hamburg, Hamburg,  
16 Germany

17 <sup>8</sup> School of Environmental Sciences, University of East Anglia, Norwich Research Park, Norwich, NR4 7TJ,  
18 UK

19 <sup>9</sup> Centre for Environment, Fisheries and Aquaculture Science, Pakefield Rd, Lowestoft, UK

20 \* Corresponding author Tel.: +1-301-385-6206; [akeshta@umd.edu](mailto:akeshta@umd.edu)

21 **Abstract**

22 Salt marshes provide various ecosystem functions and services including flooding protection, wildlife  
23 habitats, and carbon storage. These functions and services could, however, be strongly impacted by  
24 anthropogenic activities such as livestock grazing – a common practice in the Wadden Sea salt marshes located  
25 in North of Germany. To assess the impact of grazing on soil parameters, a total number of eight soil cores (Ø:  
26 18 cm; L: 50 cm) were collected in areas with and without livestock grazing, and scanned using a Computed  
27 Tomography (CT) to characterize soil parameters including soil macroporosity, sediment density, and pores  
28 connectivity. Subsequently, sub-samples were taken for determination of soil moisture content (%) and bulk

29 density ( $\text{g cm}^{-3}$ ). To account for the impact of grazing on soil drainage after tidal inundations, water table  
30 relative to soil surface was monitored during two flooding events. Our results demonstrated that grazed salt  
31 marsh has higher top-soil bulk density, and lower macroporosity and pore connectivity, than ungrazed marsh,  
32 due to soil compaction by livestock grazing. Moreover, grazed marsh has slower water drainage and that might  
33 keep the soil waterlogged for a longer period of time which has implications on lowering decomposition rate  
34 due to lower soil redox. This study provides evidence that grazing alters physical soil parameters in salt marsh.  
35 Consequently, grazing needs to be accounted for when evaluating how land use impacts ecosystem services and  
36 functions including carbon sequestration.

### 37 **Keywords**

38 Grazing, salt marsh; soil ecosystem services; Wadden Sea; computed tomography; soil macroporosity

### 39 **1. Introduction**

40 Coastal salt marshes make up the transition zone between the land and the sea, and over the last decades,  
41 this ecosystem has increasingly been recognized for its valuable ecosystem services, in particular in regards to  
42 its ability to sequester “blue carbon” and thus mitigate global climate change (Eid et al., 2017; Gedan et al.,  
43 2011; Keshta et al., 2020; Kirwan and Megonigal, 2013; Mueller et al., 2019b; Spalding et al., 2014). However,  
44 salt marshes are highly impacted by humans, for example through livestock grazing by sheep or cattle all over  
45 the world (Bakker et al., 2020; Di Bella et al., 2014; Yang et al., 2017). In some areas such as the Wadden Sea  
46 in northwestern Europe, livestock grazing has a long tradition and can be traced back as far as the bronze age  
47 “4900-800 BC” (Lotze et al., 2005). Livestock grazing alters the salt marsh ecosystem and its ecosystem  
48 services (Davidson et al., 2017; Mueller et al., 2017). It has direct effects in terms of defoliation, reducing the  
49 height of the vegetation (Bakker et al., 2020; Kiehl et al., 1996), which can lead to reduced rates of sediment  
50 deposition (Neuhaus et al., 1999). Yet, the effect of livestock grazing on the marshes ability to capture and  
51 accrete sediment is less clear (Elschot et al., 2013; Nolte et al., 2013b).

52 Livestock grazing leads to soil compaction through trampling, which increases soil bulk density (Nolte  
53 et al., 2013b). This soil compaction has significant impact on its physicochemical properties such as lowering  
54 the hydraulic conductivity, and thereby the marshes ability to drain the water that is occasionally flooding the  
55 salt marshes (Harvey and Nuttle, 1995). This reduced drainage increases waterlogging and decreases soil  
56 aeration, which in turn lowers the redox potential of the soil, and affects the exchange and turnover of nutrients,  
57 organic matter and gasses in the soil (Keshta, 2017; Mueller et al., 2017; Schrama et al., 2013). The connectivity

58 of macropores play a crucial role for the drainage of salt marshes (Harvey and Nuttle, 1995), yet, the effect of  
59 livestock grazing on the soil macropores and their connectivity has not been quantified.

60         The three-dimensional structure of the soil including the percentage of macropores and their  
61 connectivity can be assessed in detail using Computed Tomography (CT) scanning. This technology targets a  
62 broad range of key parameters relevant for soil science including soil density (Petrovic et al., 1982), grain-size  
63 distribution (Homberg et al., 2009; Munkholm et al., 2012; Taina et al., 2008), macropore structures and  
64 porosity (Anderson et al., 1990; Homberg et al., 2012; Rozenbaum et al., 2012), and micromorphology (Taina et  
65 al., 2008). Several CT-devices including medical-CT (Luo et al., 2010; Mooney et al., 2012), micro-CT  
66 (Homberg et al., 2012) and synchrotron-CT (Khan et al., 2012; Rozenbaum et al., 2012; Zong et al., 2015) could  
67 be used to analyze these parameters. Water pathways carrying nutrients through the soil pores (micro and  
68 macropores) enhance the understanding of hydrological subsurface in salt marsh (Hu et al., 2018) and that has  
69 greater impact on ecosystem service and functions. Within salt marsh research, the application of CT is rather  
70 new, but was recently applied for porosity measurements and pore network characterizations to compare natural  
71 and restored salt marshes (Dale et al., 2019; Spencer et al., 2017; Van Putte et al., 2019), as well as root and  
72 rhizome visualization (Davey et al., 2011; Spencer et al., 2017; Wigand et al., 2016).

73         To understand how livestock grazing affects soil parameters in salt marshes, and how it impacts  
74 drainage of marsh soils, we conducted CT on soil cores from two long-term (about 30 years) grazing  
75 experiments in the Wadden Sea. The experiments took place in two individual marshes, each having a grazed  
76 and an ungrazed area allowing for direct comparison. The three-dimensional structure of key soil parameters,  
77 such as density, macroporosity and pore connectivity, was visualized using CT scanning. Furthermore, CT result  
78 findings were interpreted in relation to soil drainage (i.e. travel of the water through the soil). We hypothesize  
79 (1) grazing to increase soil density and decrease soil connectivity and macroporosity. As a consequence of the  
80 grazing effect on soil parameters, we hypothesize (2) grazed marshes have slower drainage rate.

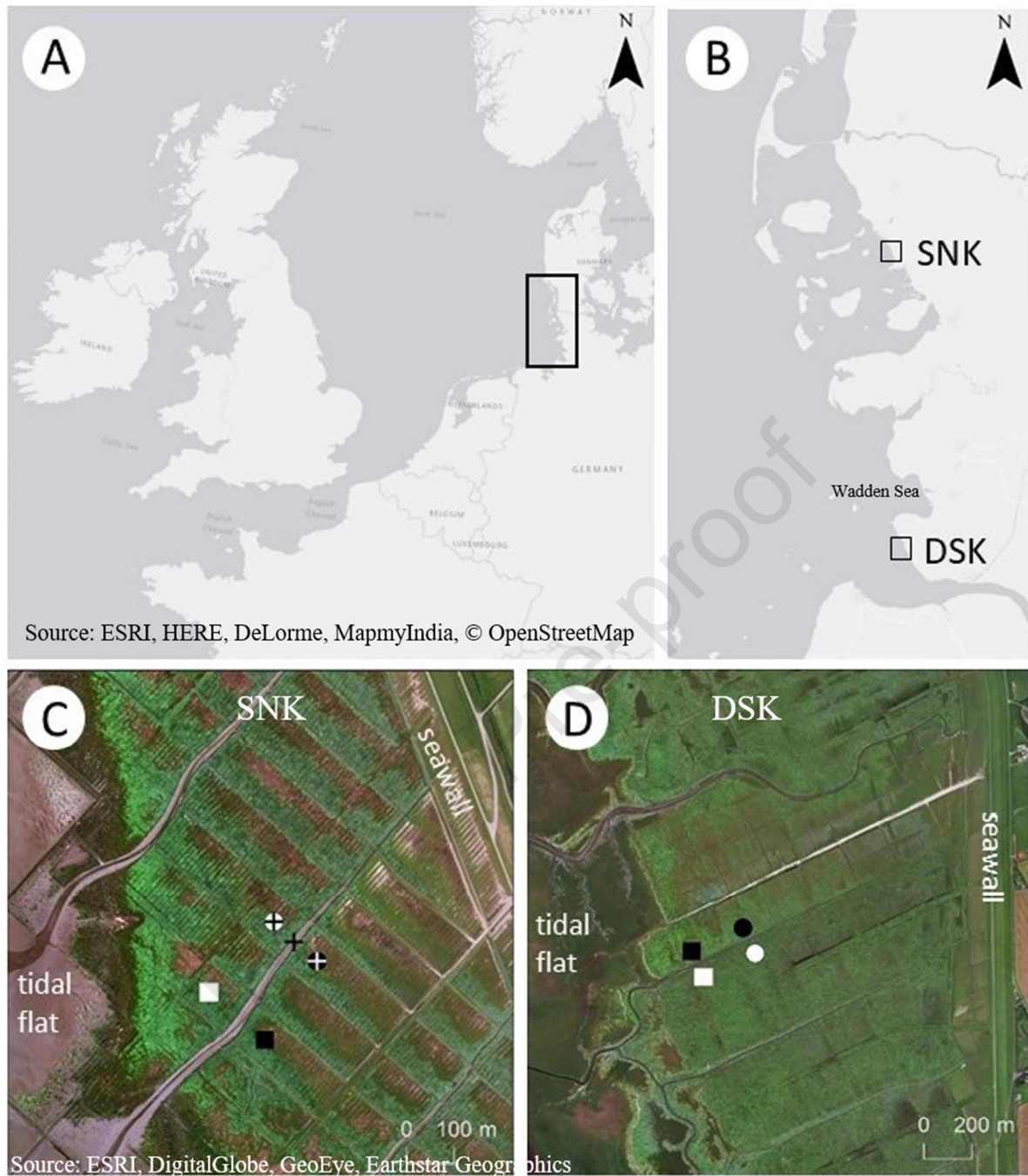
## 81 **2. Material and methods**

### 82 *2.1. Study sites*

83         The study was conducted on the mainland coast in the Schleswig-Holstein Wadden Sea National Park in the  
84 North of Germany (Fig. 1A). The area is characterized by a long history of human interventions, such as the  
85 construction of ditched sedimentation fields with brushwood groynes to enhance sedimentation (Mueller et al.,  
86 2019a) and high stocking density grazing (Esselink et al., 2009). The establishment of the National Park in

1985 led to a reduction of sheep grazing. To understand how this change in management would affect the ecosystem, long-term grazing experiments were installed in the late 1980s (Kiehl et al., 1996). Two of these sites, namely the Dieksanderkoog (DSK) and Sönke-Nissen-Koog (SNK) are used in this study (Fig. 1B). Both sites include a sheep-grazed salt marsh area, which is separated from the ungrazed control treatment by a deep creek (Nolte et al., 2013b) that cannot be crossed by the animals (Fig. 1 C & D). The grazing pressure is unevenly distributed within the grazing treatment (Bakker et al., 2020), as the sheep prefer to stay close to the seawall, where freshwater is provided. In this study, possible effects of abandonment of grazing in the ungrazed control treatment is studied in the top 15-25 cm of the soil (soil horizon separation as showed in Fig. 2), representing soil layers established after 1985 (Nolte et al., 2013b). Deeper soil layers represent the pre-1985 situation, when the control treatment area was also grazed.

DSK (53°80'23" N, 8°53'8" E) is situated at the mouth of the Elbe Estuary and is characterized by a tidal range of 3 m. Elevation above mean high tide (MHT) of the studied area ranges between 0.29 m and 0.78 m. DSK is a very wide marsh with a distance of approximately 2300 m between the seaward marsh edge and the seawall. The mean accretion rate for the past 30 years based on <sup>137</sup>Cs dated cores was found to be between 0.61 cm yr<sup>-1</sup> and 1.04 cm yr<sup>-1</sup> (Nolte et al., 2013b). Due to this high sediment supply, the marsh has been expanding over the past decades. SNK (54°38'4" N, 8°50'2" E) is located 75 km north of the DSK. The tidal range at this site is slightly higher with 3.4 m and elevation above MHT ranges between 0.41 to 0.48 m. The distance between the seaward marsh edge and the seawall is approximately 1000 m. Accretion rates are lower than at DSK and range from 0.54 cm yr<sup>-1</sup> to 0.89 cm yr<sup>-1</sup> (Nolte et al., 2013b). After the cessation of grazing, the vegetation community in the ungrazed control of both sites changed from short-growing *Puccinellia maritima* (SNK) or *Festuca rubra* (DSK) to the tall and biomass rich late successional *Elymus athericus*. The grazed treatment in SNK is still dominated by *Puccinellia maritima*, while at DSK, *Festuca rubra* and *Elymus athericus* are found in the grazed treatment (Kiehl et al., 2001; Nolte et al., 2013a).



110

111 **Fig. 1.** (A) Map of the North Sea with the study area in the Wadden Sea of Germany. (B) The Wadden Sea coast  
 112 of Schleswig-Holstein with the position of the two study sites Sönke-Nissen Koog (SNK) and Dieksanderkook  
 113 (DSK). Satellite photo of the SNK (C) and DSK (D) site. The core sampling positions are indicated. White  
 114 symbols show ungrazed and black symbols indicate grazed treatments. Landward sites are represented as circles  
 115 and seaward sites as squares. Position of three water-level sensors in SNK is additionally indicated by crosses.

## 116 2.2. Soil core sampling and collection

117 In October 2017, soil cores were collected at both sites using sharp-edge PVC-pipes with a diameter of  
 118 18 cm and gently inserted in the marsh soil to a depth of 50 cm – with gentle hammering applied as appropriate.



119 Soil was excavated around the pipe in order to retrieve the core with slight soil disturbance and compaction (less  
120 than 1 cm difference was observed between soil level inside and outside of the core). Four soil cores were  
121 collected from each site with two cores from the grazed and ungrazed treatments, respectively (Fig. 1 C & D).  
122 Within each treatment, one of the two cores was collected closer to the seawall ('landward') and the other one  
123 was collected at a greater distance to the seawall ('seaward') in order to elucidate spatial differences within  
124 treatments. This results in a total number of eight soil cores, which were wrapped with plastic to prevent drying  
125 and water loss, and immediately brought to the laboratory for further analysis. In this study, we used the  
126 accretion rate data provided in (Nolte et al., 2013b) for assessing the soil depth corresponding to the start of  
127 grazing experiment in both DSK and SNK.

### 128 2.3. CT scanning

129 The cores were kept in the PVC pipes and scanned using a Toshiba Aquilion 64™ Computed  
130 tomography (CT) scanner at the hospital Klinikum Bremen-Mitte, with an X-ray source voltage of 120 kV and a  
131 current of 600 mA. The CT scans have a resolution of 0.351 mm in x- and y-direction and 0.5 mm resolution in  
132 z-direction. The z-direction represents the depth along the core axes, while x and y are perpendicular to the core  
133 axes (reconstruction interval: 0.3 mm). Images were reconstructed using Toshiba's patented helical cone beam  
134 reconstruction technique. The obtained CT data were processed using the Amira ZIB edition software version  
135 2017.39 (Stalling et al., 2005; <http://amira.zib.de>). The PVC pipes, together with about 2 mm of the core rims,  
136 were removed from the CT data in order to discard marginal artefacts resulting from the coring process. The  
137 scans were visualized in 3D, separating three key soil components by threshold segmentation; 1) sediment ( $\geq 20$   
138 HU; HU: Hounsfield units; a quantitative scale for radio-density"), 2) water/root-filled pores ( $\geq 980$  HU and  
139  $< 20$  HU) and 3) air-filled pores ( $< -980$  HU). Subsequently, the following soil parameters were identified and/or  
140 calculated for each of the soil cores: air-filled and water/root-filled pores, pore connectivity index, and soil  
141 macroporosity and density (estimated based on the X-ray attenuation of the soil) (Anderson et al., 1990).

### 142 2.4. Processing of CT-scan images

143 Image analyses allowed for quantification of key parameters in the soil representing depth profiles  
144 averaging over the 234 cm<sup>2</sup> core area. Pore and soil volumes were identified and quantified using the Material  
145 Statistics-module (*volume per slice*) and used for calculation of soil macroporosity (only pores  $> 10$  mm<sup>3</sup> were  
146 visualized and presented). The extension of individual pores in the soil were identified applying the 'Connected  
147 Components'-module, which identifies connected pores in 3D. The identified pores were subsequently  
148 parameterized with the Shape Analysis module to visualize all pores, while only pores  $> 10$  mm<sup>3</sup> are presented to

149 reduce image overwhelming. Number of disconnected pores divided by total pore volume within each slice  
150 were used as a semiquantitative proxy for soil permeability (degree of soil pore connectivity ‘hereafter: pore  
151 connectivity index’). In this case, soils with high connectivity index had fewer distinct pores, because most of  
152 the pores were connected, which was represented by a low value in the connectivity index. In contrast, soils with  
153 low connectivity had more distinct pores because pores were disconnected, which were represented by high  
154 value in the connectivity index. The X-ray attenuation (HU) was used as a proxy for wet soil bulk density. To  
155 avoid the impact of the core margins, all the segmented soil was reduced by 3 voxels and calculated its mean  
156 value in X-ray attenuation in every xy-oriented CT-Slice, followed by using the mean value determined with the  
157 *Statistics per slice per label* algorithm of the Material Statistics-module of the segmented soil. Voxels with a  
158 value higher than 1000 (HU) were considered outliers and discarded from the analyses. The soil macroporosity  
159 was visualized by applying the ‘AverageValueInNeighborhood’-module using a cube volume of about 1 cm<sup>3</sup>  
160 (31 × 31 × 31 isotropic voxel) on segmentation data in which all pores were represented by the value 1 and soil  
161 by the value 0. For the visualization of soil density, the ‘Average Value In Neighborhood’-module was applied  
162 on the segmented soil - using a cube volume of about 1 cm<sup>3</sup>.

### 163 2.5. Soil analyses

164 After CT scanning, soil cores were opened along the side and soil samples were taken at five  
165 centimeters intervals using standard soil sample rings ( $\varnothing=53$  mm, depth = 5 cm ; Eijkelkamp). The rings were  
166 pushed into the side of the core to 7 cm depth to avoid sampling the core edges. Samples were stored in plastic  
167 bags at 4 °C and were processed within few days from sampling. Soil samples were dried at 105 °C to a constant  
168 weight and weighed to quantify soil bulk density (g cm<sup>-3</sup>) and soil moisture content (%) based on weight loss.  
169 For soil particle size analyses, the soil cores were opened by sawing the PVC tube in halves and revealing soil  
170 core from inside. Half of the core was carefully removed to enable visual inspection of stratigraphy where layers  
171 appear in different shades of grey; one is lighter and one is darker. Hence, we refer to these as “light” and “dark”  
172 layers. Distinct light and dark layers were observed and samples (5 g) were collected from ten of these. In order  
173 to test for difference in soil composition between layers, soil samples were collected from the dark and light  
174 layers in the soil cores and analyzed for grain-size distribution. Particle-size measurements (McGregor et al.,  
175 2009) were performed in the Particle-Size Laboratory at MARUM, University of Bremen with a Beckman  
176 Coulter Laser Diffraction Particle Size Analyzer LS 13320 (soil samples preparation with detailed methods are  
177 available in the supplementary material).

### 178 2.6. Hydrology

179 To assess the effect of grazing on water drainage, change of water level relative to soil surface was  
180 measured in the landward position of SNK. Here, three pressure sensors (type 'Micro-Diver', Eijkelkamp) were  
181 deployed in three monitoring wells covering both the grazed and ungrazed treatment as well as a tidal creek  
182 (Fig. 1C), which was used to record the reference water levels. The monitoring wells for ungrazed and grazed  
183 were located approximately 48 m from nearest tidal creek (Fig. 1C). The wells consisted of perforated PVC-  
184 tubes surrounded by fabric to prevent clay and silt from collecting in the well. Pressure sensors inside the wells  
185 were installed below the marsh surface level (45-50 cm from marsh soil surface). An additional pressure sensor  
186 was installed close by on the mainland to record air pressure for compensation (type 'Baro-Diver', Eijkelkamp).  
187 Measurements were recorded at five minute intervals in autumn 2016, while data presented (Fig. 8) are  
188 corresponding to two events inundating the entire marsh platform of SNK were recorded on 08.08.2016 and  
189 28.09.2016, respectively.

### 190 2.7. Statistical analyses

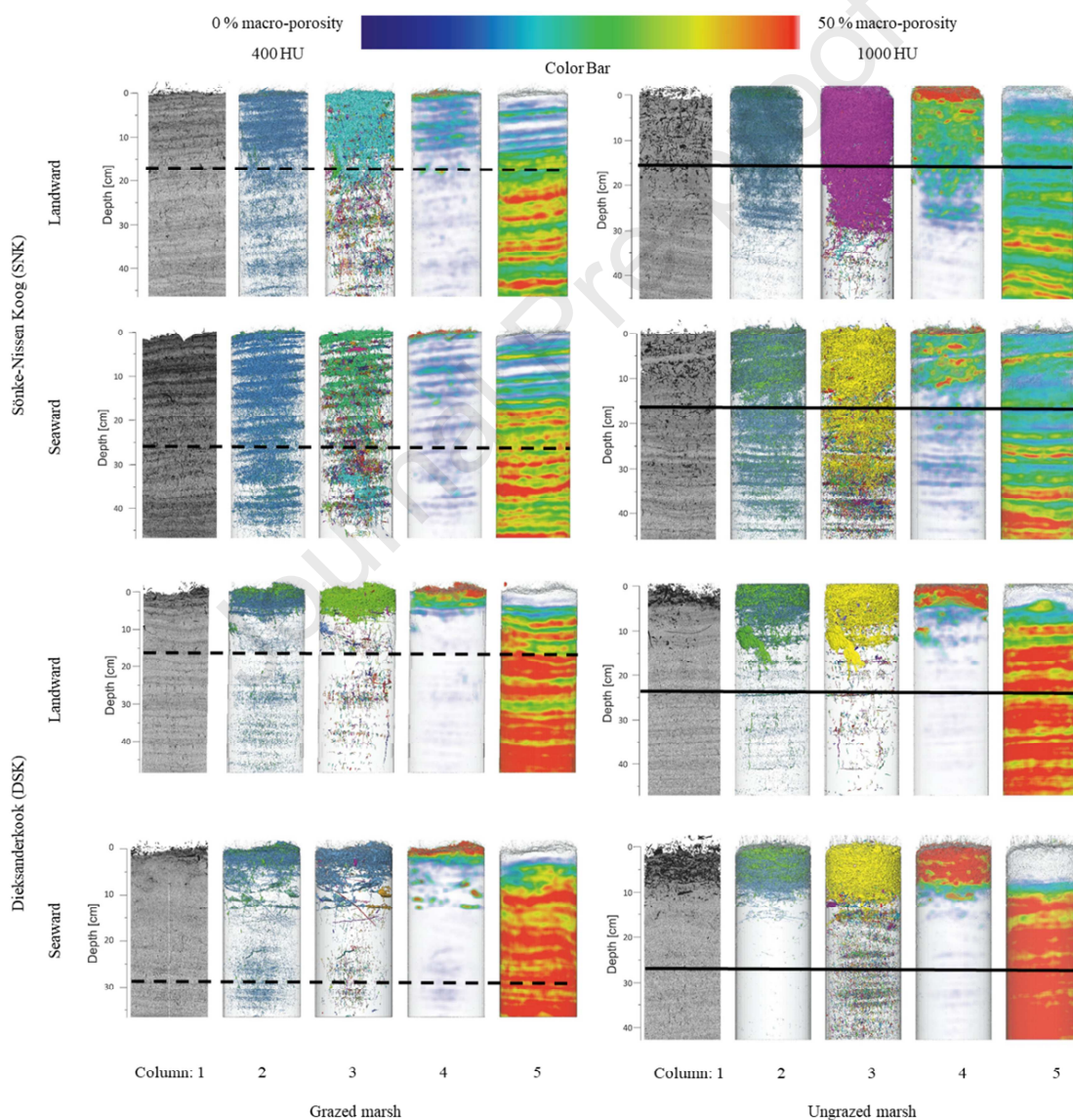
191 Soil samples were grouped into two categories: top soil (0-20 cm) and bottom soil (deeper than 20 cm).  
192 Over soil depth, repeated measure ANOVA was used to test the main effects of treatment (grazed vs ungrazed)  
193 and position (landward vs seaward) on the soil bulk density and moisture content for the top and bottom soils  
194 separately (Supplement 1). Data were found to be normally distributed with homogeneous variances and data  
195 used for presentation are mean  $\pm$  SE unless otherwise noted. Tukey's post-hoc test was used to examine the least  
196 significant difference between the means. All statistical analyses were performed using SAS 9.4.

## 197 3. Results

### 198 3.1. Visualization of soils parameters using CT scans

199 Central CT-slice of the core (Fig. 2: column 1) showed clear stratification in soil layers (dark vs light  
200 layers). In the SNK landward grazed core, a clear horizon separation for all parameters (Fig. 2: columns 2-5)  
201 was found at 15 cm. In contrast, in SNK landward ungrazed core, a clear horizon separation was found at 35 cm,  
202 demonstrating difference in soil pores, macroporosity, and density between the grazed and ungrazed treatments.  
203 In the SNK seaward grazed core, the horizons were less clear, but a horizon separation was detected at 20 cm,  
204 most pronounced for density (Fig. 2: column 5). In the SNK seaward ungrazed core, connectivity index (Fig. 2:  
205 column 3) and density (Fig. 2: column 5) showed a horizon separation at 38 cm. Comparing SNK grazed and  
206 ungrazed treatments in general, it is noteworthy that connectivity index tended to be higher in the ungrazed  
207 treatment, and air-filled pores were almost exclusively found in the ungrazed treatment. Moreover, air-filled

208 pores were more frequently present at seaward compared to landward salt marsh. In the DSK landward grazed  
 209 core, there was a horizon separation for all parameters (Fig. 2: column 2-5) at 8 cm. By contrast, in the DSK  
 210 landward ungrazed core, a clear horizon separation was found at 13 cm, demonstrating difference between the  
 211 grazed and ungrazed treatment. In the DSK seaward grazed core, a clear horizon for all soil parameters (Fig. 2:  
 212 column 2-5) was found at 4 cm. By contrast, in the DSK-seaward ungrazed core, a clear horizon separation was  
 213 found at 12 cm. Comparing DSK grazed and ungrazed treatments in general, it is noteworthy that the ungrazed  
 214 treatment had higher pore connectivity index and macroporosity than the grazed treatments. Moreover, air-filled  
 215 pores tended to have higher occurrence in the ungrazed core soil profile.



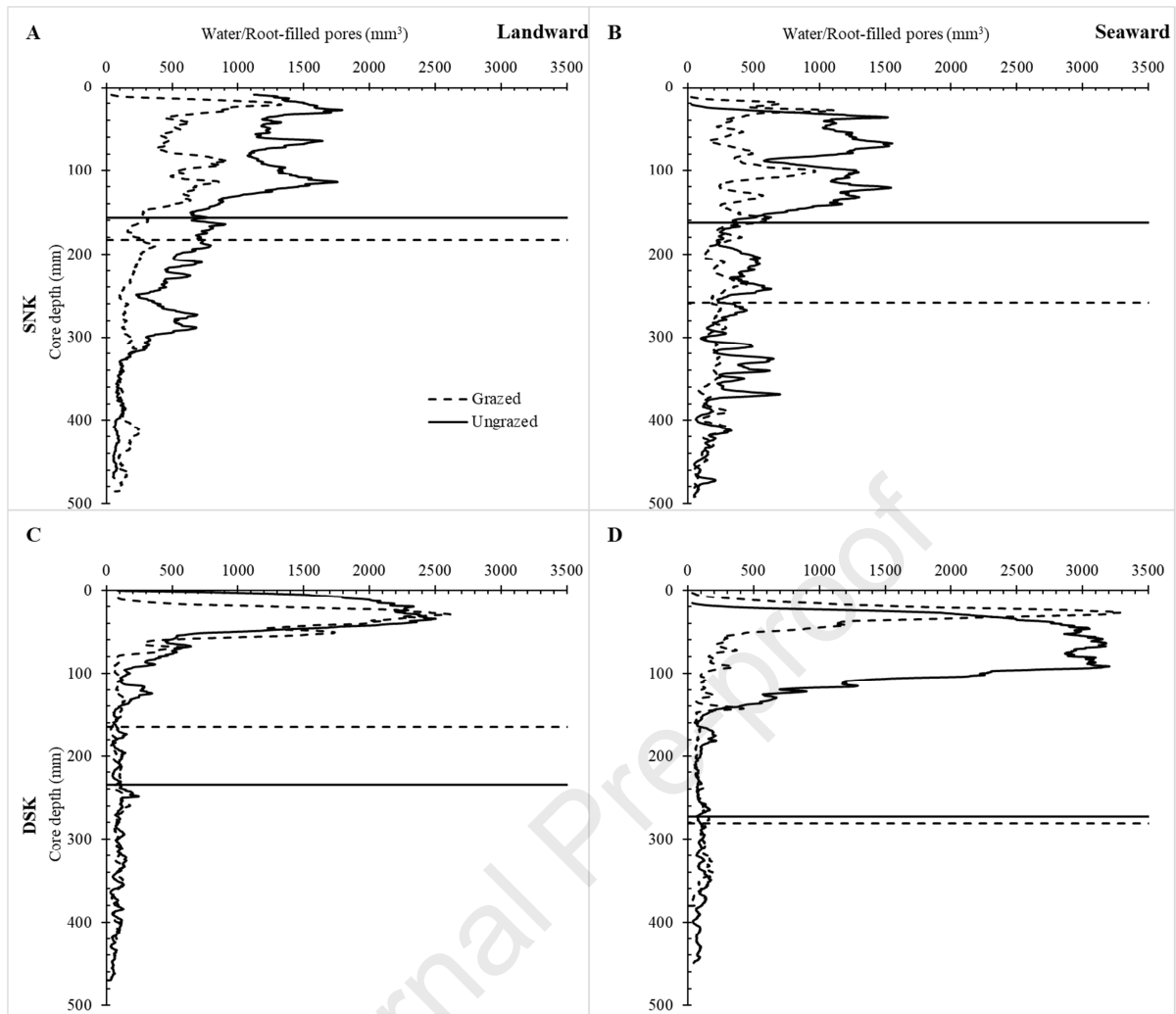
216

217 **Fig. 2.** Three-dimensional (3D) visualization of key soil parameters obtained from CT scan images processed  
 218 with AMIRA software. The following parameters were visualized: column 1: 2D central CT slice of soil core, 2:

219 pores air-filled (green) and water- and/or root-filled (blue), 3: pore connectivity index (same color: connected  
220 pores, different colors: disconnected pores per same column), 4: macroporosity where dense red color means  
221 higher porosity (0% for blue/transparent and 50% for red), and 5: soil density where dense red color means  
222 higher sediment density (400 HU for blue/transparent and 1000 HU for red). Horizontal punctuated and solid  
223 lines represent the depth corresponding to the start of grazing experiment in the grazed and ungrazed treatment,  
224 respectively.

### 225 3.2. Water/root-filled pores

226 In SNK, the depth profiles for water/root-filled pores differed between grazed and ungrazed treatments,  
227 showing a higher volume of water/root-filled pores in the ungrazed treatment (Fig. 3 A). High pore-water  
228 volume was characteristic for the topsoil. Water/root pore volume was particularly high in the top soil of the  
229 ungrazed treatment. At greater depth (below 20 cm), the profiles were overlapping and representing the situation  
230 in the past, when both treatments were equally grazed. There were no pronounced differences between the  
231 landward and seaward positions in pore volume. In DSK, water/root pore volume was higher in the top 0-10 cm.  
232 In the seaward position, a high volume was detected down to 15 cm in the ungrazed treatment, whereas high  
233 volume was detected down to 5 cm in the grazed treatment. In the landward position, no pronounced difference  
234 in water/root-filled pore volume was found between the grazed and ungrazed treatments. However, it was higher  
235 in the topsoil of DSK than in SNK, and at depth (<15 cm) the water/root-filled pore volume was lower in DSK  
236 than in SNK.



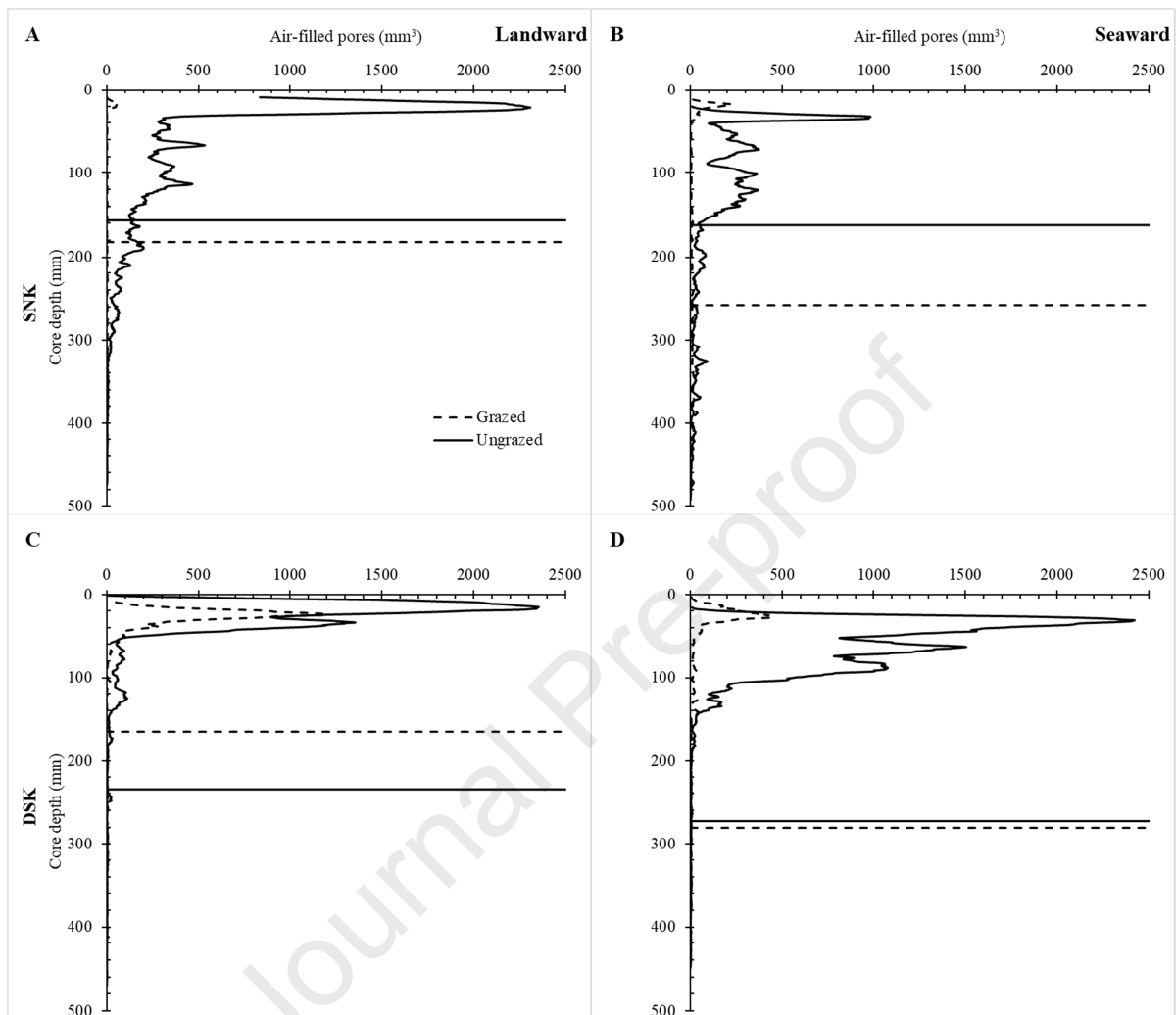
237

238 **Fig. 3.** Depth profiles of water/root-filled pores volume ( $\text{mm}^3$ ) derived from CT-scans. Horizontal punctuated  
 239 and solid lines represent the depth corresponding to the start of grazing experiment in the grazed and ungrazed  
 240 treatment, respectively.

### 241 3.3. Air-filled pores

242 In SNK, the depth profiles for air-filled pores volume differed between the grazed and ungrazed treatment  
 243 (Fig. 4). Air-filled pores were almost exclusively present in the ungrazed treatment, where air-filled pores were  
 244 detected down to 15 cm, coinciding with the time when grazing was terminated in the ungrazed treatment. In the  
 245 grazed treatment, a small amount of air-filled pores was observed in the top 4 cm, it was, however, smaller than  
 246 in the ungrazed treatment. No marked differences between the landward and seaward positions were found in  
 247 air-filled pores. In DSK, air-filled pores were observed in both the grazed and ungrazed treatment. However, in  
 248 the grazed treatment air-filled pores were restricted to the top-5 cm, whereas air-filled pores were found down to

249 15 cm in the ungrazed treatment. No clear differences between the landward and seaward positions were  
 250 detected for air-filled pores at DSK.



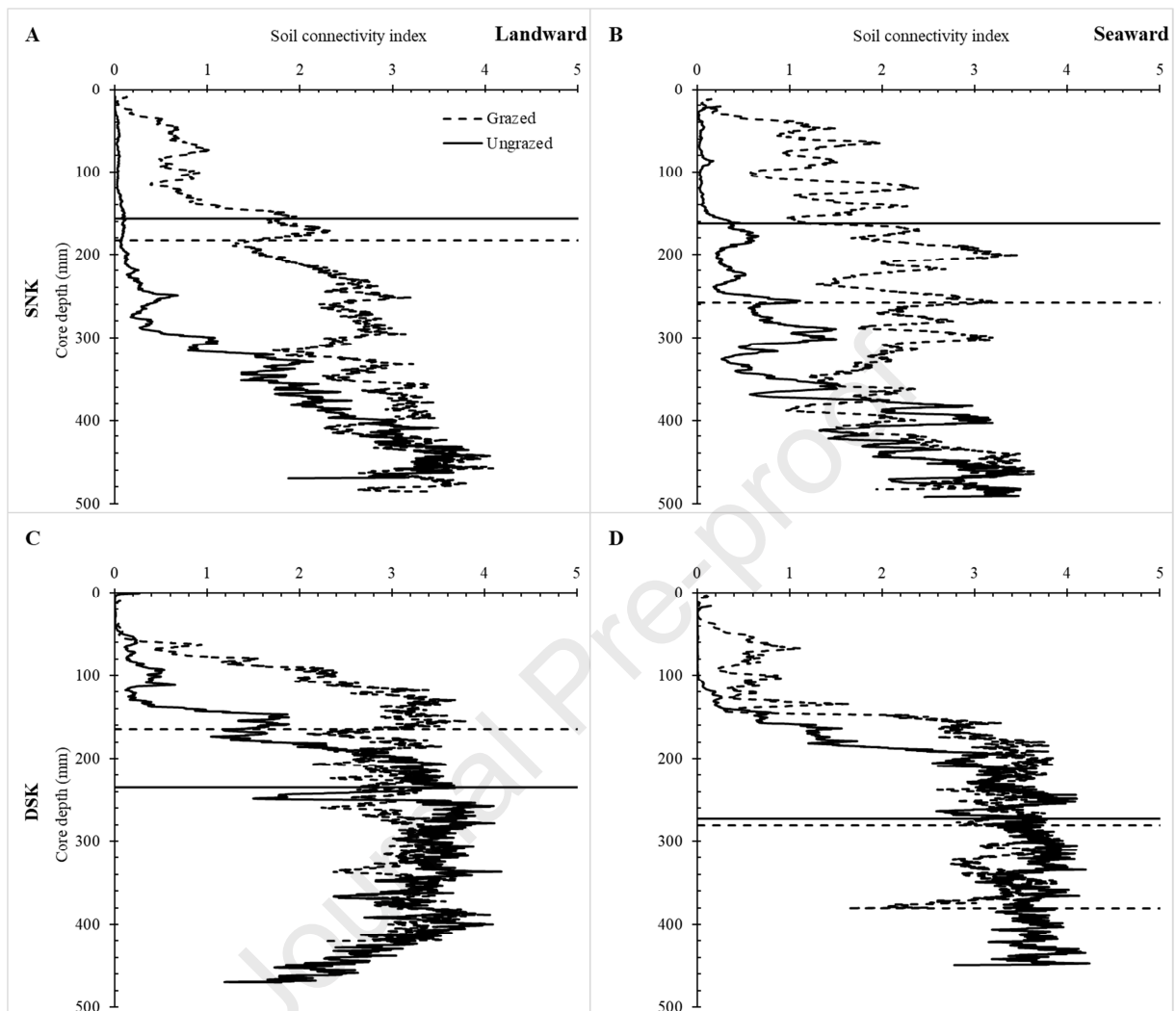
251

252 **Fig. 4.** Depth profiles of air-filled pores volume ( $\text{mm}^3$ ) derived from CT-scans. Horizontal punctuated and solid  
 253 lines represent the depth corresponding to the start of grazing experiment in the grazed and ungrazed treatment,  
 254 respectively.

### 255 3.4. Pore connectivity index as a proxy for pore permeability

256 Pore permeability is semi-quantitatively measured and represented as connectivity index (Fig. 5) stating the  
 257 number of individual pores relative to the total pore volume. Here, low values represent high connectivity with  
 258 a well-connected network of soil pores. In SNK, the ungrazed treatment showed a higher connectivity (low  
 259 values) in the top 35 cm of the cores than grazed treatment. In contrast, below 35 cm, connectivity of grazed and  
 260 ungrazed treatments was similar. In DSK, the depth profiles for pore connectivity differed between the grazed

261 and ungrazed treatments in the top 20 cm of the cores showing higher pore connectivity in the ungrazed than  
 262 grazed treatments. In contrast, below 20 cm, connectivity index of grazed and ungrazed treatments was similar.



263

264 **Fig. 5.** Depth profiles of connectivity index used as a proxy for pore permeability derived from CT-scans.

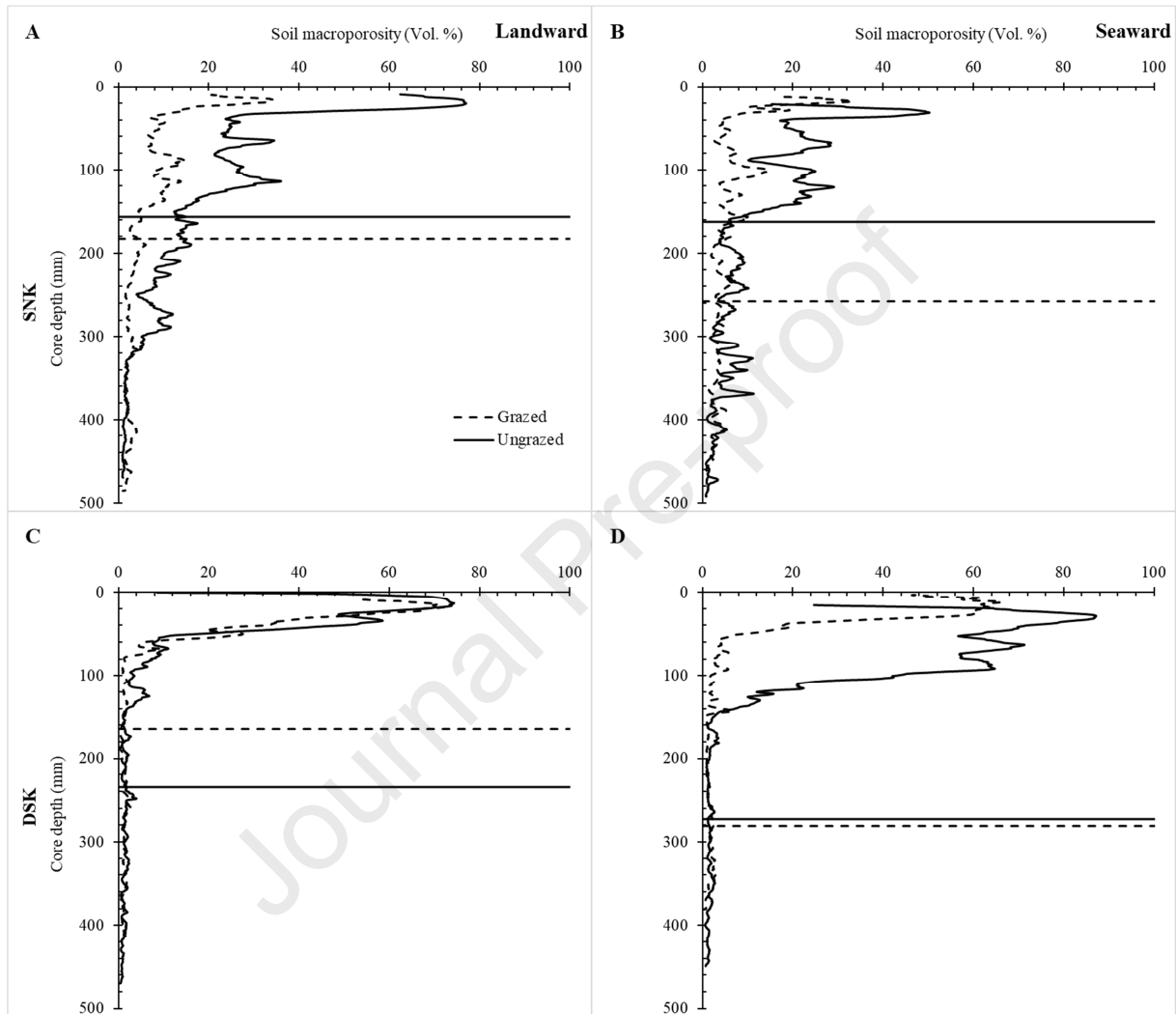
265 Horizontal punctuated and solid lines represent the depth corresponding to the start of grazing experiment in the  
 266 grazed and ungrazed treatment, respectively.

### 267 3.5. Soil macroporosity

268 In SNK, the depth profiles for macroporosity differed between the grazed and ungrazed treatments  
 269 showing a higher macroporosity in the topsoil (top 20 cm) of the ungrazed treatment (Fig. 6). At greater depth  
 270 (below 20 cm), the profiles for grazed and ungrazed treatments were more similar representing the situation  
 271 prior to 1985, where both treatment areas were evenly grazed. There were no pronounced differences between  
 272 the landward and seaward positions in macroporosity. In DSK, higher soil macroporosity was observed in the



273 top soil only (10-15 cm soil depth) in both landward and seaward position, while bottom soil (deeper than 20  
 274 cm) showed very low soil macroporosity (lower than 5 %). In DSK landward, no marked differences between  
 275 soil macroporosity in grazed and ungrazed marshes, while DSK seaward ungrazed marsh has higher soil  
 276 macroporosity than grazed marsh noticeable in the top 15 cm only.



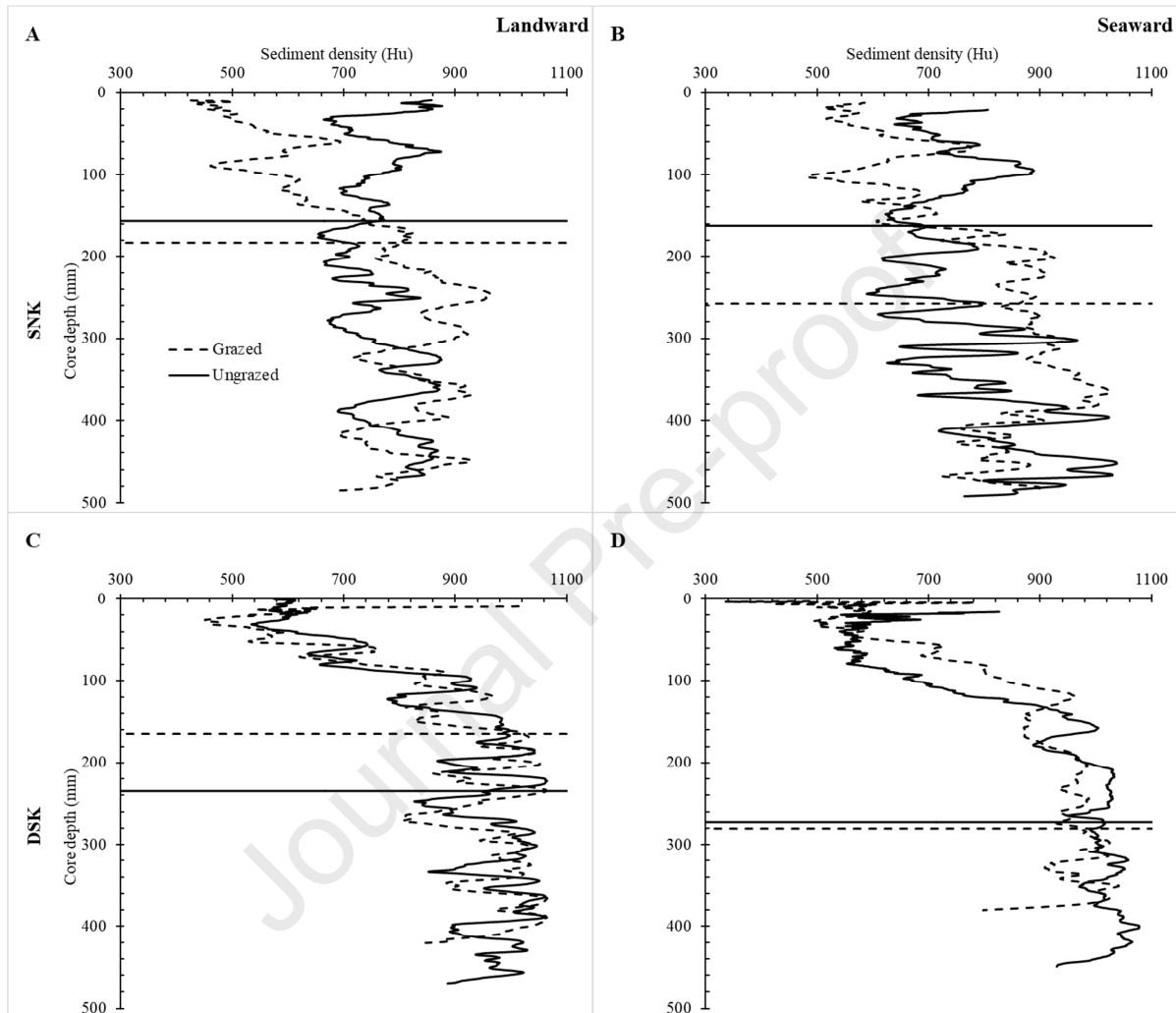
277

278 **Fig. 6.** Depth profiles of soil macroporosity (Vol. %) derived from CT-scans. Horizontal punctuated and solid  
 279 lines represent the depth corresponding to the start of grazing experiment in the grazed and ungrazed treatment,  
 280 respectively.

### 281 3.6. Soil density based on X-ray attenuation

282 In SNK landward and seaward positions (Fig. 7A and 7B) and at the top 8 cm only, the ungrazed treatment  
 283 had a higher soil density than the grazed treatment since SNK site receives more sediment and has different  
 284 vegetation composition, however, at 10-20 cm soil depth, soil in the grazed treatment was more dense than in

285 the ungrazed treatment which similar to results presented in supplement 1 where top soil, in general, is more  
 286 dense in grazed than ungrazed marsh. At the seaward DSK position (Fig. 7D), we found the grazed treatment to  
 287 have a higher soil density at depth 5-15 cm, while at the landward position (Fig. 7C), differences in soil density  
 288 between grazed and ungrazed treatments were not obvious.



289

290 **Fig. 7.** Depth profiles of the soil density derived from CT-scans; x-ray attenuation (HU) is used as a proxy for  
 291 soil density. Horizontal punctuated and solid lines represent the depth corresponding to the start of grazing  
 292 experiment in the grazed and ungrazed treatment, respectively.

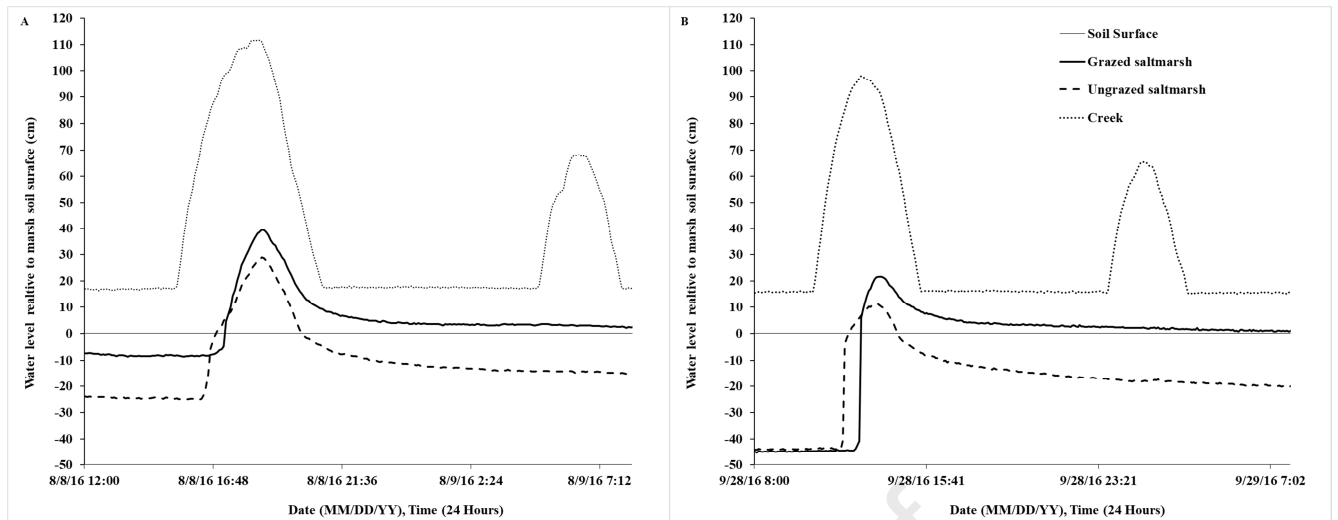
### 293 3.7. Soil physical parameters

294 Grazing had a significant effect on top soil bulk density (supplement 1,  $F = 196.04$ ,  $P = 0.045$ ) where  
 295 grazed treatments had higher soil bulk densities than ungrazed treatments ( $0.92 \pm 0.09$  and  $0.79 \pm 0.10$   $\text{g cm}^{-3}$  for  
 296 landward positions, respectively, and  $0.99 \pm 0.11$  and  $0.84 \pm 0.12$   $\text{g cm}^{-3}$  for seaward positions, respectively,  
 297 supplement 1A). The core stratigraphies showed clearly visible dark and light layers (Supplement 2A), which

298 correspond with the layers observed in the CT images (Fig 2. Column 1-5). For instance, at seaward grazed  
299 saltmarsh at SNK, light layer appear at soil depth of 10 cm (column 1 at Fig. 2.) which correspond to lower soil  
300 density (Fig. 2 column 5) at the same depth. Light layer has higher sand content than dark layer and these  
301 alternations in the sediment conditions are event-driven, primarily by storms bringing in and depositing larger  
302 portions of coarse grained suspended material, than during normal tidal interactions. A larger proportion of fine  
303 sands was found in the light layers than in the darker layers. The dark layers had a larger proportion of smaller  
304 grained silts and clays. The alternation in grain-size distribution supports that the stratification is event-driven.  
305 Layering is found in both the grazed and ungrazed marshes showing that stratification was unaffected by  
306 grazing.

### 307 *3.8. Hydrology*

308 In our study, the two time events presented at Fig. 8 are during spring tide (8 August, 2016 corresponds to  
309 the 5<sup>th</sup> day of lunar cycle & 28 September, 2016 corresponds to the 27<sup>th</sup> of the lunar cycle). During these two  
310 events, both marsh surfaces were flooded with water and hence, we are comparing them after the flooding took  
311 place. Water level relative to soil surface is presented in Fig. 8. On 08.08.2016 prior to tidal flooding, the water  
312 table was at -23 cm in the ungrazed and at -9 cm in the grazed treatment. After high tide, water drained slightly  
313 faster from the ungrazed treatment, falling below the soil surface level within about 1.5 hours. After 6 hours, the  
314 water table had reached a relatively stable level of -15 cm in the ungrazed treatment, whereas the water table  
315 was still above the soil surface in the grazed treatment. On 28.09.2016 prior to the tidal flooding, the water table  
316 was at -43 cm in both the grazed and ungrazed treatments. After high tide, water drained slightly faster from the  
317 ungrazed treatment, falling below the soil surface level within 1 hour. After 6 hours, the water table had reached  
318 a level of -17 cm in the ungrazed treatment, whereas the water table remained above the soil surface at 1 cm in  
319 the grazed treatment for a longer time. In general, the hydrological observations showed a higher water drainage  
320 rate in the ungrazed treatment compared to the grazed treatment.



321

322 **Fig. 8.** Water level relative to soil surface at the landward position of SNK during 08.08.2016 (A) and  
 323 28.09.2016 (B). Lines, including the creek, represent the water level relative to soil surface (0 cm).

#### 324 4. Discussion

325 In our study, the use of the CT scan technique for saltmarsh cores enabled the analyses of soil  
 326 parameters including soil pore permeability and macroporosity in three-dimensional way. In line with our first  
 327 hypothesis, the results indicate that livestock grazing in salt marshes decrease soil macroporosity (Fig. 2:  
 328 column 4) and increase top soil density (supplement 1). As a result of less permeability represented by less  
 329 connected soil pores, water drained slower under livestock grazing as expected based on our second hypothesis.

##### 330 4.1. Application of CT-scanning in salt marshes

331 CT-scanning allows for visualization and quantification of key soil parameters in salt marshes. The 3D  
 332 visualization facilitates a visual comparison of individual cores, which allow of observation of the spatial  
 333 variation in soil parameters. Recently, characterization and quantification of soil physical parameters in a non-  
 334 destructive approach has gained high focus from saltmarsh researchers using CT scanning for obtaining high  
 335 image resolution (mm to  $\mu\text{m}$ ). A major issue in applying CT to salt marsh, or soils in general, is the sample size  
 336 and the respective voxel size of the obtained CT scan. Besides its methodological limitations, CT imaging offers  
 337 a powerful tool to improve our understanding of soil textures and components in three dimensions, and allow  
 338 consequently a better evaluation of soil behavior and processes (Taina et al., 2008).

339 In this study, CT clearly demonstrated a spatial variation in soil horizons (Fig. 2) due to change in  
 340 grazing practices, and marked layered structure of key soil parameters (Fig. 2 and supplement 2), due to event

341 driven deposition of material. In this study average values were calculated over a large cross-sectional area  
342 covering 243 cm<sup>2</sup> of soil core capturing and accounting for the natural variation in the marsh soil. This is a clear  
343 advantage over more destructive methods depending on core slicing and/or subsampling, which disturb the soil  
344 structure. In this study, the non-descriptive nature of the CT-scanning rendered an analysis of the pore  
345 connectivity (Fig. 5) showing higher connectivity in ungrazed soils, and thereby a better drainage rate, which  
346 was confirmed by a subsequent drainage study (Fig. 8). A major advantage of medical-CT is the operator-  
347 independent image acquisition. In contrast to micro and synchrotron CT-devices, all medical-CT devices are  
348 calibrated to Hounsfield-units, which provide a principal comparability of the obtained data from various  
349 devices (Cnudde and Boone, 2013). However, differences might still occur due to differences in resolution and  
350 or reconstruction software. During data processing, the most critical operation is the segmentation, usually based  
351 on thresholding, of the various components of interest. However, as long as similar objects of similar size are  
352 measured with the same device, resolution, and applied threshold, the errors are constant and allow their  
353 comparison. Another limitation for CT scanning is the *partial volume effect* which must be taken into account  
354 (Cnudde and Boone, 2013), which signifies that a voxel value is the mean of the x-ray attenuation over the  
355 complete voxel volume. Only a combined approach using referenced subsamples of various size from a soil  
356 sample being measured with the respective CT devices would allow to capture a soil in its entire complexity.

#### 357 4.2. Effects of grazing on physical soil parameters

358 Grazing led to lower soil permeability, lower macroporosities, and higher top soil densities (Column 3,  
359 4, and 5 in Fig. 2 and supplement 1A). This is consistent with the outcome of previous grazing experiments in  
360 the Wadden Sea that have demonstrated a significant impact of grazing on soil parameters (Elschot et al., 2013;  
361 Nolte et al., 2013b) and redox chemistry (Bakker et al., 2020; Mueller et al., 2017). Many of these studies argue  
362 that trampling leads to soil compaction, which reduces water drainage and thus the availability of oxygen in the  
363 soil. Soil redox potential often used as indication for the oxygen availability in the soil with lower values as an  
364 indication for prolonged period of waterlogging (Mitsch and Gosselink, 2007), which is a result for soil  
365 compaction and blocking the water pathway through soil pores. In our study, trampling by sheep led to denser  
366 and more compacted soils (Supplement 1), which is similar to findings from other temperate and tropical  
367 marshes (Haines-Young and Potschin, 2010; Tanentzap and Coomes, 2012). CT scanning in our study allowed  
368 for a specific focus on pore connectivity in the soil, which facilitates the vertical flow of water and thereby  
369 water drainage of the salt marsh. The results clearly show that permeability (Fig. 5) and macroporosity (Fig. 6)  
370 is lower with grazing, particularly, in the top profile of the soil cores. As a result of mechanical stresses that

371 have been added to the soil surface, grazing can alter the physical and chemical nature of the soil, and that may  
372 negatively impact the ecosystems services and functions provided by saltmarshes including blue C storage  
373 (Davidson et al., 2017; Mueller et al., 2019a), however some studies reported that the impact of grazing on blue  
374 C storage is minimal on a broader-scale (Harvey et al., 2019).

#### 375 *4.3. Differences in physical soil parameters between landward and seaward locations in salt marshes*

376 Our results showed that grazing had a stronger impact on landward compared to seaward positions.  
377 Grazing practices had an impact on soil compaction (Supplement 1) and soil horizons formation as noticed in  
378 SNK salt marshes located at landward position (Fig 2), where the grazed marshes showed higher soil density at  
379 the upper soil profile (0-15 cm) compared with the ungrazed marshes. This pattern can be explained by the  
380 grazing behavior of livestock. For cattle, behavioral studies in salt marshes have shown a grazing intensity  
381 gradient, with a decreasing local grazing intensity with increasing distance to the freshwater source located close  
382 to the seawall (Esselink et al., 2002; Nolte et al., 2013b). A similar behavior in sheep is seen as the cause for an  
383 observed gradient in vegetation height at SNK (Bakker et al., 2020). Consequently, the landward marsh is more  
384 exposed to grazing from livestock animals, leading to more trampling and soil compaction, and this is the course  
385 of the lower macro-porosity and connectivity shown at the landward marsh (Column 4, and 5 in Fig. 2).

#### 386 *4.4. Effect of grazing on salt marsh drainage*

387 The marsh hydrology measurements demonstrated that water drains slower in the grazed salt marsh  
388 (Fig. 8). This observation is supported by our CT-scans showing lower water/root-filled pore volumes (Fig. 3)  
389 and lower soil pore permeability in the grazed marsh (Fig. 5), leading to lower drainage rates. This is further  
390 explained by the observations of air-filled pores (Fig. 4), which almost exclusively were found in the ungrazed  
391 marsh. This provides evidence that sheep grazing lowers drainage of the salt marsh and cause longer periods of  
392 waterlogging. Our findings of higher bulk density in top soil (Supplement 1) and lower water/root-filled pore  
393 volume in the grazed marsh (Fig. 3) suggests that compaction of the soil, due to trampling by the sheep, is  
394 responsible for the altered hydrological conditions. These observations are supported by previous research in  
395 salt marshes reporting a positive correlation between soil macroporosity and their ability to let water travel  
396 through (Van Putte et al., 2019), and compaction of soil as a result of trampling leading to low drainage rate and  
397 higher surface runoff (Gifford and Hawkins, 1979).

#### 398 *4.5. Implications and outlook*

399           The results of our study may have implications for ecosystem functions and services delivered by salt  
400 marshes in general and in particular at the Wadden Sea. As we found grazing having pronounced impacts on soil  
401 physical structure and on drainage rate, our results are relevant for future management strategies of salt  
402 marshes, particularly in regard to carbon sequestration, which is one of the most important ecosystem services  
403 of salt marshes (Kirwan and Megonigal, 2013; McLeod et al., 2011). The low drainage rate of the grazed marsh  
404 allow the marsh soil to stay waterlogged for a longer period of time. This play a significant role in marsh  
405 lowering oxygen availability and redox potential, altering the microbial community and organic matter turnover  
406 and thereby increasing their carbon sequestration capacity. While our study supports the evidence that grazing  
407 may enhance carbon sequestration rate in grazed saltmarsh by altering the soil redox after prolonged water  
408 logging, it is however still unclear if continuous aboveground biomass removal and lower plant productivity as a  
409 result of grazing will counterpart the lower carbon turnover rate which is a crucial part for assessing net carbon  
410 sequestration rates.

## 411 **5. Conclusion**

412           Salt marsh grazing by sheep decreased macroporosity and pore connectivity due to compaction  
413 lowering the pore space, which also increased the top soil density. Marsh hydrology was impacted by grazing  
414 resulting in slower water drainage after inundations, resulting from low drainage after tidal inundation caused by  
415 lower pore volume and connectivity keeping the soil waterlogged for a longer period of time. Our current results  
416 demonstrated that livestock grazing in salt marsh at SNK and DSK had an impact on soil parameters leading to  
417 lower pore connectivity and macroporosity. These grazing implications have greater direct and indirect impact  
418 on ecosystem services and functions provided by salt marsh at the Wadden Sea including carbon sequestration  
419 and excess nutrients removal.

## 420 **Acknowledgements**

421           We would like to thank Dr. Martin Stock and the Administration of the Wadden Sea National Park  
422 Schleswig-Holstein for allowing us to access the sites and take samples. This research was partly funded by the  
423 Bauer-Hollmann Foundation in the framework of the project INTERFACE. The authors would like to  
424 acknowledge the Society of Wetland Scientists (SWS) and Department of Environmental Science and  
425 Technology at the University of Maryland College Park - USA for their funding support for the Wetland  
426 Ambassador Fellowship awarded to the first author during which he conducted the research at Hamburg  
427 University – Germany. JT acknowledges funding by the DFG Research Center/Cluster of Excellence “MARUM

428 – The Ocean in the Earth System”. Klinikum Bremen-Mitte and Prof. Dr. Arne-Jörn Lemke and Christian  
429 Timann are thanked for providing their facilities and supporting the performed computed tomography  
430 measurements. For KkJ, the research was funded in part by The Helmholtz Climate Initiative (HI-CAM). HI-  
431 CAM is funded by the Helmholtz Association's Initiative and Networking Fund. The authors are responsible for  
432 the content of this publication. The authors would like to acknowledge the reviewers whose comments helped to  
433 improve the quality of the manuscript.

#### 434 References

- 435  
436 Anderson, S.H., Peyton, R.L., Gantzer, C.J., 1990. Evaluation of constructed and natural soil macropores using  
437 X-ray computed tomography. *Geoderma* 46, 13-29.
- 438 Bakker, J.P., Schrama, M., Esselink, P., Daniels, P., Bhole, N., Nolte, S., de Vries, Y., Veeneklaas, R.M., Stock,  
439 M., 2020. Long-Term Effects of Sheep Grazing in Various Densities on Marsh Properties and Vegetation  
440 Dynamics in Two Different Salt-Marsh Zones. *Estuaries and Coasts* 43, 298-315.
- 441 Cnudde, V., Boone, M.N., 2013. High-resolution X-ray computed tomography in geosciences: A review of the  
442 current technology and applications. *Earth-Science Reviews* 123, 1-17.
- 443 Dale, J., Cundy, A.B., Spencer, K.L., Carr, S.J., Croudace, I.W., Burgess, H.M., Nash, D.J., 2019. Sediment  
444 structure and physicochemical changes following tidal inundation at a large open coast managed realignment  
445 site. *Science of The Total Environment* 660, 1419-1432.
- 446 Davey, E., Wigand, C., Johnson, R., Sundberg, K., Morris, J., Roman, C.T., 2011. Use of computed tomography  
447 imaging for quantifying coarse roots, rhizomes, peat, and particle densities in marsh soils. *Ecological*  
448 *Applications* 21, 2156-2171.
- 449 Davidson, K.E., Fowler, M.S., Skov, M.W., Doerr, S.H., Beaumont, N., Griffin, J.N., 2017. Livestock grazing  
450 alters multiple ecosystem properties and services in salt marshes: a meta-analysis. *Journal of Applied Ecology*  
451 54, 1395-1405.
- 452 Di Bella, C.E., Jacobo, E., Golluscio, R.A., Rodríguez, A.M., 2014. Effect of cattle grazing on soil salinity and  
453 vegetation composition along an elevation gradient in a temperate coastal salt marsh of Samborombón Bay  
454 (Argentina). *Wetlands Ecology and Management* 22, 1-13.
- 455 Eid, E.M., Keshta, A.E., Shaltout, K.H., Baldwin, A.H., El-Din, S., Ahmed, A., 2017. Carbon sequestration  
456 potential of the five Mediterranean lakes of Egypt. *Fundamental and Applied Limnology/Archiv für*  
457 *Hydrobiologie* 190, 87-96.

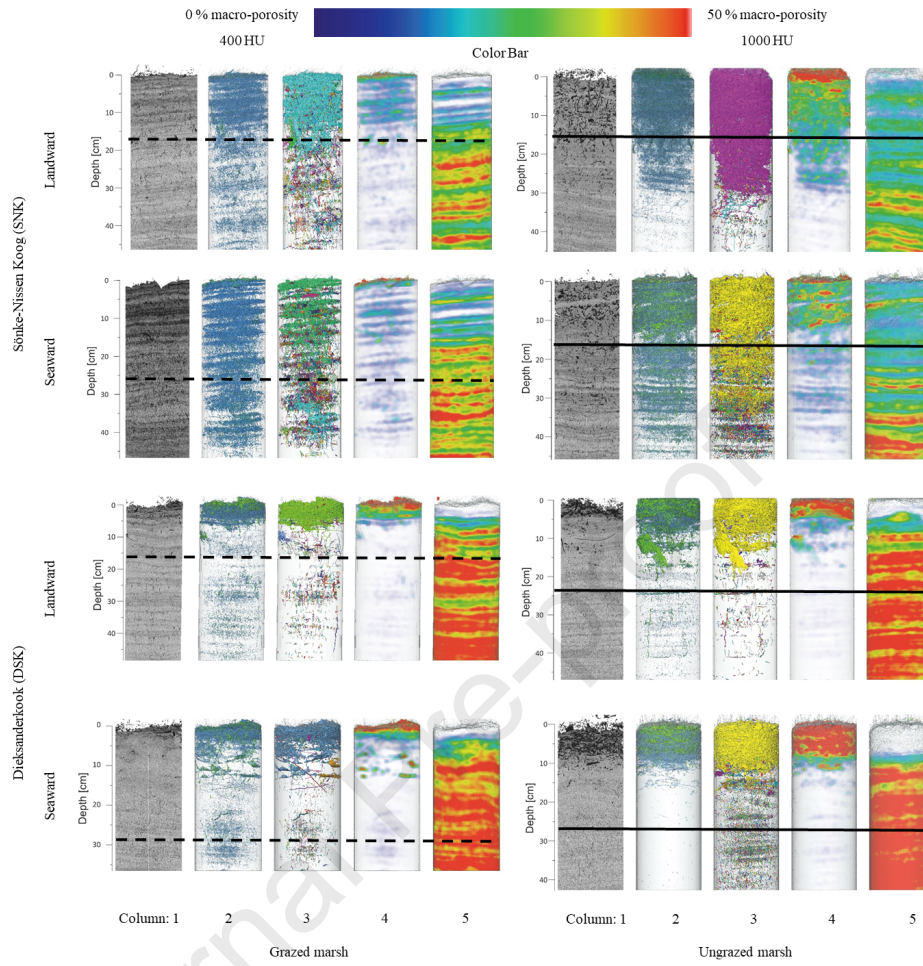


- 458 Elschot, K., Bouma, T.J., Temmerman, S., Bakker, J.P., 2013. Effects of long-term grazing on sediment  
459 deposition and salt-marsh accretion rates. *Estuarine Coastal and Shelf Science* 133, 109-115.
- 460 Esselink, P., Fresco, L.F.M., Dijkema, K.S., 2002. Vegetation change in a man-made salt marsh affected by a  
461 reduction in both grazing and drainage. *Applied Vegetation Science* 5, 17-32.
- 462 Esselink, P., Petersen, J., Arens, S., Bakker, J.P., Bunje, J., Dijkema, K.S., Hecker, N., Hellwig, U., Jensen,  
463 A.V., Kers, A.S., Körber, P., Lammerts, E.J., Stock, M., Veeneklaas, R.M., Vreeken, M., Wolter, M., 2009. Salt  
464 Marshes. Thematic Report No. 8, in: Marencic, H., Vlas, J.d. (Eds.), *Quality Status Report 2009. Wadden Sea*  
465 *Ecosystem No. 25. Common Wadden Sea Secretariat, Trilateral Monitoring and Assessment Group,*  
466 *Wilhelmshaven, Germany.*
- 467 Gedan, K.B., Kirwan, M.L., Wolanski, E., Barbier, E.B., Silliman, B.R., 2011. The present and future role of  
468 coastal wetland vegetation in protecting shorelines: answering recent challenges to the paradigm. *Climatic*  
469 *Change* 106, 7-29.
- 470 Gifford, G.F., Hawkins, R.H., 1979. DETERMINISTIC HYDROLOGIC MODELING OF GRAZING  
471 SYSTEM IMPACTS ON INFILTRATION RATES. *Water Resources Bulletin* 15, 924-934.
- 472 Haines-Young, R., Potschin, M., 2010. The links between biodiversity, ecosystem services and human well-  
473 being. *Ecosystem Ecology: a new synthesis* 1, 110-139.
- 474 Harvey, J.W., Nuttle, W.K., 1995. Fluxes of water and solute in a coastal wetland sediment. 2. Effect of  
475 macropores on solute exchange with surface water. *Journal of Hydrology* 164, 109-125.
- 476 Homberg, U., Baum, D., Prohaska, S., Kalbe, U., Witt, K.J., 2012. Automatic extraction and analysis of realistic  
477 pore structures from muCT data for pore space characterization of graded soil, ICSE6 - 6th International  
478 conference on scour and erosion (Proceedings), ICSE6-181 ed, pp. 345-352.
- 479 Homberg, U., Binner, R., Prohaska, S., Dercksen, V., Kuß, A., Kalbe, U., 2009. Determining geometric grain  
480 structure from x-ray micro-tomograms of graded soil, in: Witt, K.J., Schanz, T. (Eds.), *Workshop Internal*  
481 *Erosion. Bauhaus-Universität*, pp. 37-53.
- 482 Hu, X., Li, Z.C., Li, X.Y., Wang, P., Zhao, Y.D., Liu, L.Y., Lu, Y.L., 2018. Soil Macropore Structure  
483 Characterized by X-Ray Computed Tomography Under Different Land Uses in the Qinghai Lake Watershed,  
484 Qinghai-Tibet Plateau. *Pedosphere* 28, 478-487.
- 485 Keshta, A.E., Shaltout, K.H., Baldwin, A.H., El-Din, A.A.S., 2020. Sediment clays are trapping heavy metals in  
486 urban lakes: An indicator for severe industrial and agricultural influence on coastal wetlands at the  
487 Mediterranean coast of Egypt. *Marine Pollution Bulletin* 151, 110816.

- 488 Keshta, A.E.S.S., 2017. Hydrology, Soil Redox, and Pore-Water Iron Regulate Carbon Cycling in Natural and  
489 Restored Tidal Freshwater Wetlands in the Chesapeake Bay, Maryland, USA.
- 490 Khan, F., Enzmann, F., Kersten, M., Wiegmann, A., Steiner, K., 2012. 3D simulation of the permeability tensor  
491 in a soil aggregate on basis of nanotomographic imaging and LBE solver. *Journal of Soils and Sediments* 12,  
492 86-96.
- 493 Kiehl, K., Eischeid, I., Gettner, S., Walter, J., 1996. Impact of different sheep grazing intensities on salt marsh  
494 vegetation in northern Germany. *Journal of Vegetation Science* 7, 99-106.
- 495 Kiehl, K., Esselink, P., Gettner, S., Bakker, J.P., 2001. The Impact of Sheep Grazing on Net Nitrogen  
496 Mineralization Rate in Two Temperate Salt Marshes. *Plant Biology* 3, 553-560.
- 497 Kirwan, M.L., Megonigal, J.P., 2013. Tidal wetland stability in the face of human impacts and sea-level rise.  
498 *Nature* 504, 53.
- 499 Lotze, H.K., Reise, K., Worm, B., van Beusekom, J., Busch, M., Ehlers, A., Heinrich, D., Hoffmann, R.C.,  
500 Holm, P., Jensen, C., Knottnerus, O.S., Langhanki, N., Prummel, W., Vollmer, M., Wolff, W.J., 2005. Human  
501 transformations of the Wadden Sea ecosystem through time: a synthesis. *Helgoland Marine Research* 59, 84-95.
- 502 Luo, L., Lin, H., Li, S., 2010. Quantification of 3-D soil macropore networks in different soil types and land  
503 uses using computed tomography. *Journal of Hydrology* 393, 53-64.
- 504 McGregor, H.V., Dupont, L., Stuu, J.B.W., Kuhlmann, H., 2009. Vegetation change, goats, and religion: a  
505 2000-year history of land use in southern Morocco. *Quaternary Science Reviews* 28, 1434-1448.
- 506 McLeod, E., Chmura, G.L., Bouillon, S., Salm, R., Bjork, M., Duarte, C.M., Lovelock, C.E., Schlesinger, W.H.,  
507 Silliman, B.R., 2011. A blueprint for blue carbon: toward an improved understanding of the role of vegetated  
508 coastal habitats in sequestering CO<sub>2</sub>. *Frontiers in Ecology and the Environment* 9, 552-560.
- 509 Mitsch, W.J., Gosselink, J.G., 2007. *Wetlands*. Wiley, Hoboken, NJ.
- 510 Mooney, S.J., Pridmore, T.P., Helliwell, J., Bennett, M.J., 2012. Developing X-ray Computed Tomography to  
511 non-invasively image 3-D root systems architecture in soil. *Plant and Soil* 352, 1-22.
- 512 Mueller, P., Do, H.T., Jensen, K., Nolte, S., 2019a. Origin of organic carbon in the topsoil of Wadden Sea salt  
513 marshes. *Marine Ecology Progress Series* 624, 39-50.
- 514 Mueller, P., Granse, D., Nolte, S., Do, H.T., Weingartner, M., Hoth, S., Jensen, K., 2017. Top-down control of  
515 carbon sequestration: grazing affects microbial structure and function in salt marsh soils. *Ecological*  
516 *Applications* 27, 1435-1450.

- 517 Mueller, P., Ladiges, N., Jack, A., Schmiendl, G., Kutzbach, L., Jensen, K., Nolte, S., 2019b. Assessing the long-  
518 term carbon-sequestration potential of the semi-natural salt marshes in the European Wadden Sea. *Ecosphere*  
519 10, e02556.
- 520 Munkholm, L.J., Heck, R.J., Deen, B., 2012. Soil pore characteristics assessed from X-ray micro-CT derived  
521 images and correlations to soil friability. *Geoderma* 181-182, 22-29.
- 522 Neuhaus, R., Stelter, T., Kiehl, K., 1999. Sedimentation in salt marshes affected by grazing regime,  
523 topographical patterns and regional differences. *Senckenbergiana maritima* 29, 113-116.
- 524 Nolte, S., Esselink, P., Bakker, J.P., 2013a. Flower production of *Aster tripolium* is affected by behavioral  
525 differences in livestock species and stocking densities: the role of activity and selectivity. *Ecological Research*  
526 28, 821-831.
- 527 Nolte, S., Müller, F., Schuerch, M., Wanner, A., Esselink, P., Bakker, J.P., Jensen, K., 2013b. Does livestock  
528 grazing affect sediment deposition and accretion rates in salt marshes? *Estuarine, Coastal and Shelf Science* 135,  
529 296-305.
- 530 Petrovic, A.M., Siebert, J.E., Rieke, P.E., 1982. Soil Bulk Density Analysis in Three Dimensions by Computed  
531 Tomographic Scanning I. *Soil Science Society of America Journal* 46, 445-450.
- 532 Rozenbaum, O., Bruand, A., Le Trong, E., 2012. Soil porosity resulting from the assemblage of silt grains with  
533 a clay phase: New perspectives related to utilization of X-ray synchrotron computed microtomography.  
534 *Comptes Rendus Geoscience* 344, 516-525.
- 535 Schrama, M., Heijning, P., Bakker, J.P., van Wijnen, H.J., Berg, M.P., Olf, H., 2013. Herbivore trampling as an  
536 alternative pathway for explaining differences in nitrogen mineralization in moist grasslands. *Oecologia* 172,  
537 231-243.
- 538 Spalding, M.D., McIvor, A.L., Beck, M.W., Koch, E.W., Möller, I., Reed, D.J., Rubinoff, P., Spencer, T.,  
539 Tolhurst, T.J., Wamsley, T.V., van Wesenbeeck, B.K., Wolanski, E., Woodroffe, C.D., 2014. Coastal  
540 Ecosystems: A Critical Element of Risk Reduction. *Conservation Letters* 7, 293-301.
- 541 Spencer, K.L., Carr, S.J., Diggens, L.M., Tempest, J.A., Morris, M.A., Harvey, G.L., 2017. The impact of pre-  
542 restoration land-use and disturbance on sediment structure, hydrology and the sediment geochemical  
543 environment in restored saltmarshes. *Science of The Total Environment* 587-588, 47-58.
- 544 Stalling, D., Westerhoff, M., Hege, H.-C., 2005. Amira: A highly interactive system for visual data analysis.  
545 *The visualization handbook* 38, 749-767.

- 546 Taina, I.A., Heck, R.J., Elliot, T.R., 2008. Application of X-ray computed tomography to soil science: A  
547 literature review. *Canadian Journal of Soil Science* 88, 1-19.
- 548 Tanentzap, A.J., Coomes, D.A., 2012. Carbon storage in terrestrial ecosystems: do browsing and grazing  
549 herbivores matter? *Biological Reviews* 87, 72-94.
- 550 Van Putte, N., Temmerman, S., Verreydt, G., Seuntjens, P., Maris, T., Heyndrickx, M., Boone, M., Joris, I.,  
551 Meire, P., 2019. Groundwater dynamics in a restored tidal marsh are limited by historical soil compaction.  
552 *Estuarine, Coastal and Shelf Science*, 106101.
- 553 Wigand, C., Sundberg, K., Hanson, A., Davey, E., Johnson, R., Watson, E., Morris, J., 2016. Varying  
554 Inundation Regimes Differentially Affect Natural and Sand-Amended Marsh Sediments. *PLOS ONE* 11,  
555 e0164956.
- 556 Yang, Z., Nolte, S., Wu, J., 2017. Tidal flooding diminishes the effects of livestock grazing on soil micro-food  
557 webs in a coastal saltmarsh. *Agriculture, Ecosystems & Environment* 236, 177-186.
- 558 Zong, Y., Yu, X., Zhu, M., Lu, S., 2015. Characterizing soil pore structure using nitrogen adsorption, mercury  
559 intrusion porosimetry, and synchrotron-radiation-based X-ray computed microtomography techniques. *Journal*  
560 *of Soils and Sediments* 15, 302-312.
- 561



### Highlights

- Investigating soil cores using minimally non-destructive X-ray CT analysis allows identification of soil parameters in undisturbed soil zones
- Grazed salt marshes have lower soil macroporosity and higher density than ungrazed salt marshes
- Ungrazed salt marshes have higher drainage rate than grazed saltmarshes

Journal Pre-proof

**Declaration of interests**

The authors declare that they have no known competing financial interests or personal relationships that could have appeared to influence the work reported in this paper.

The authors declare the following financial interests/personal relationships which may be considered as potential competing interests:

Journal Pre-proof